Sensors & Actuators: B. Chemical 300 (2019) 127001

Contents lists available at ScienceDirect

Sensors and Actuators B: Chemical

journal homepage: www.elsevier.com/locate/snb

Sandwich-type signal-off photoelectrochemical immunosensor based on dual suppression effect of PbS quantum dots/Co_3O_4 polyhedron as signal amplification for procalcitonin detection

Yanrong Qian[a], Jinhui Feng[a], Huan Wang[a], Dawei Fan[a], Na Jiang[a,*], Qin Wei[a,*], Huangxian Ju[a,b]

[a] Key Laboratory of Interfacial Reaction & Sensing Analysis in Universities of Shandong, School of Chemistry and Chemical Engineering, University of Jinan, Jinan 250022, China

[b] State Key Laboratory of Analytical Chemistry for Life Science, Department of Chemistry, Nanjing University, Nanjing 210023, China

ARTICLE INFO

Keywords:
Photoelectrochemical immunosensor
Dual suppression effect
Procalcitonin
Signal-off

ABSTRACT

A novel signal-off photoelectrochemical (PEC) immunosensor was proposed for procalcitonin (PCT) sensitive detection based on the Au nanoparticles/BiOI nanosheets/Black TiO_2 nanoparticles (Au NPs/BiOI NSs/B-TiO_2 NPs) as photoactive matrix and PbS quantum dots/Co_3O_4 polyhedron (PbS/Co_3O_4) as a quenching signal label for signal amplification. Concretely, BiOI NSs was fabricated by successive ionic layer absorption and reaction (SILAR) and formed the interlaced flake-like structure. Then Au NPs dropped on the BiOI NSs/B-TiO_2 NPs electrode forming Au NPs/BiOI NSs/B-TiO_2 NPs sensitization structure, which increased the utilization of visible light and accelerated electron transfer rate, resulting in a desirable PEC signal. PbS/Co_3O_4, an effective dual suppression signal quencher, was proposed for signal-off PEC immunosensor to weaken the photocurrent response because of the steric impedance, competitive absorption of light and competing consumption of electron donor. In this proposal, PCT was chosen to measure the performance of the suggested PEC immunosensor. Consequently, the fabricated PEC immunosensor showed a widely detection ranged from 0.1 pg/mL to 50 ng/mL and a low detection limit of 0.02 pg/mL (S/N = 3). What is more, the proposed PEC immunosensor possessed satisfactory selectivity, stability and reproducibility.

1. Introduction

Procalcitonin (PCT) recently has considered as the most prospective inflammatory marker for bacterial infections on account of high sensitivity to the severity of sepsis [1]. The level of PCT elevated when suffering from sepsis, multiple organ failure or serious infection of bacteria, fungi, or parasites [2]. PCT is effective indicator of early diagnosis for the bacterial inflammatory diseases. Currently, radioactive immunoassay, enzyme-linked fluorescent assay and so forth for PCT detection face some challenges in sensitivity, cost and operational convenience [3]. Therefore, it is of great significance to study an effectively sensitive PCT detection method.

Photoelectrochemical (PEC) immunosensor as an analytical technique shows a booming tendency due to operation handily, low cost, easy miniaturization [4–7]. Remarkably, the difference between excitation and detection forms that respectively belong to light source and electric signal provides contribution for low background and admirable sensitivity [8]. Accordingly, PEC immunosensor has attracted extensive interest in tremendous potential for detecting all kinds of targets [9,10]. As one of PEC immunosensor classic models, signal-off PEC immunosensor makes an impact for decreasing initial signal utilizing insulated immune complex and signal labels [11]. It is acknowledged that the signal-off PEC immunosensor has numerous advantages that simple structure, easy operation, and good stability [12]. Regrettably, the signal-off PEC immunosensor possesses low sensitivity compared with signal-on PEC immunosensor [13,14]. For meeting the demand of sensitivity, various signal-off amplification strategies emerge in endlessly and based on the following three modes: enzymatic reaction, steric-hindrance effect and p-n type effect [15–17]. Therein, most of reports are based on a signal change model but actually depending on two or more variational signal model is beneficial for improving the sensitivity of immunosensor [18]. Given in the enzymatic reaction needing the harsh environment and high cost, a dual suppression mode combining impedance and competition is applied to achieve signal amplification in this work.

It is noteworthy that signal labels play a hard-core role in a dual

* Corresponding authors.
E-mail addresses: chm_jiangn@ujn.edu.cn (N. Jiang), sdjndxwq@163.com (Q. Wei).

https://doi.org/10.1016/j.snb.2019.127001
Received 1 July 2019; Received in revised form 15 August 2019; Accepted 18 August 2019
Available online 19 August 2019
0925-4005/

suppression model [19]. As well known, PbS quantum dots (PbS QDs) as a p-type narrow bandgap semiconductor is an excellent quenching candidate for the absorption ranging from 400 nm to 1300 nm [20,21]. PbS QDs produce photointroduced electron-hole pairs (e^-/h^+) under the light irradiation. Furthermore, the desirable photogenerated electrons combine with the dissolved oxygen in the electrolyte, resulting in superoxide anion radicals $(O^{2-})^{\cdot}$ reacting with ascorbic acid (AA) [22]. As a result, PbS QDs form the competitive situation with photoactive matrix for the light absorption and AA, which results in the reduction of signal. In addition, carrying capacity of signal label is also a key factor affecting signal amplification [23]. In this present work, small PbS QDs possess the poor load capacity. Hence, looking for a good carrier is necessary for enhancing the signal amplification. Co_3O_4 derived from ZIF-67 with a polyhedral frame structure possesses biggish surface area, which is an all-right carrier. On the hand, Co_3O_4, a p-type semiconductor, not only as a support material to load PbS QDs and antibody but also as a hole collector to react with AA [24]. On the other hand, the steric impedance of Co_3O_4 polyhedron blocks the transfer of charge and AA [25]. Therefore, PbS/Co_3O_4 possesses the effect of steric impedance and competition enhancing the signal reduction from photoactive matrix, which is beneficial for improving the sensitivity of signal-off PEC immunosensor.

Equally important, the photoactive materials with desired signal play a pivotal role in the fabrication of PEC immunosensor [26,27]. Titanium dioxide (TiO_2) was used widely in PEC immunosensor due to its cheap, non-toxic and brilliant photocatalytic efficiency [28,29]. However, TiO_2 with wide band-gap of 3.2 eV only absorb ultraviolet region light limiting its application. Recently, Black TiO_2 was widely applied in the fields of lithium-ion rechargeable battery, fuel cell and supercapacitor because it makes up the defect of TiO_2 [30,31]. In this work, this emerging Black TiO_2 nanoparticles (B-TiO_2 NPs) was utilized for improving the utilization of light [32,33]. Moreover, the B-TiO_2 NPs increase the roughness of indium tin oxide (ITO), which is convenient for the attachment of BiOI NSs by a successive ionic layer adsorption and reaction (SILAR). The nanoarray flake structure of BiOI NSs with large specific surface area is gainful for light capture, electron transfer and providing a large number of binding sites to immobilize other substance. Simultaneously, matched band gap between BiOI NSs and B-TiO_2 NPs inhabited the recombination of photogenerated (e^-/h^+). Significantly, Au nanoparticles (Au NPs) are focused due to the localized surface plasmon resonance (LSPR), the excellent electronic and optical characteristics [34]. The Au NPs with biocompatibility and excellent stability coating on the BiOI NSs are conducive to increase the formation rate of e-/h^+ and promote the separation of photogenerated charge carriers [35]. So the addition of BiOI NSs and Au NPs greatly increases the photocurrent response of photoactive matrix.

Here, Au nanoparticles/BiOI nanosheets/Black TiO_2 nanoparticles (Au NPs/BiOI NSs/B-TiO_2 NPs) sensitization structure enhanced photocurrent under the light irradiation by increasing conductivity, capturing more light and improving photoelectric conversion efficiency for PEC immunosensor. Last but not least, PbS/Co_3O_4 was utilized as a signal label firstly through the collective effect between steric impedance and competition for light and electron donor achieving the signal amplification for the signal-off PEC immunosensor. And the proposed PEC immunosensor was measured for PCT detection in the electrolyte containing amount of AA.

2. Experimental section

2.1. Materials, reagents and apparatus

Materials, reagents and apparatus could be found in Supporting materials (SM).

2.2. Preparation of the B-TiO_2 NPs, Au NPs, TGA-PbS QDs

The synthesis of the B-TiO_2 NPs, Au NPs, TGA-PbS QDs were based on the previous literature with a little modified [36–38]. The prepared details were narrated in SM.

2.3. Preparation of PbS/Co_3O_4-Ab_2

The form of Co_3O_4 was according to the previous work with lightly modified [39]. In a typical run, first of all, ZIF-67 as a precursor was fabricated by mixing cobalt salts and 2-methylimidazole. Specifically, 2.910 g of $Co(NO_3)_2{\cdot}6H_2O$ and 13.284 g of 2-methylimidazole was respectively dissolved in 250 mL of methanol. Then, the 2-methylimidazole solution was added into the $Co(NO_3)_2$ solution under stirring. The above mixture was aged for 24 h at the room temperature. Followed by washed with the methanol and dried in a vacuum oven, the ZIF-67 was gained. Co_3O_4 was prepared by the calcination of ZIF-67under air atmosphere. The ZIF-67 was maintained at 350 °C for 2 h and the heating rate was 1 °C/min. The Co_3O_4 powder was acquired.

At first, 0.1 g of Co_3O_4 was dispersed in 10 mL ethanol solution containing 0.15 mL of 3-aminopropyltriethoxysilane. The suspension was heated at 90 °C for 24 h. After cooled to the room temperature, the above solution was washed with ethanol. Ultimately, the desired Co_3O_4-NH_2 was obtained by dried in a vacuum oven.

The details of prepared PbS/Co_3O_4 were as follows: 10 mg of aminated Co_3O_4 polyhedron was dispersed in 15 mL of TGA-PbS QDs solution containing 0.38 g of EDC and 0.055 g of NHS. Then, the mixture was stirred at room temperature for 2 h. The target product was obtained after washed with ultrapure water for several times and dried in a vacuum oven.

In order to synthesize the PbS/CO_3O_4-Ab_2, the detailed steps were narrated: Firstly, 10 μL of 5 mg/mL EDC and 10 μL of 1 mg/mL NHS were injected into 2 mL of 10 μg/mL PCT-Ab_2 solution and vibrated at 4 °C for 30 min. Secondly, 5 mg of PbS/CO_3O_4 was added into the mentioned solution and incubated at 4 °C for 12 h. Then, 100 μL of 1% wt BSA solution was added into the mixed system oscillating at 4 °C for 6 h. Eventually, the aimed product was redistributed in 2 mL of PBS after removing redundant substance through centrifugation and stored at 4 °C refrigerator for using in the future.

2.4. Construction of the sandwich-type PEC immunosensor

A sandwich-type PEC immunosensor was constructed as shown in Scheme 1. Prior to fabrication, the bare ITO glass pieces (2.0 cm × 0.8 cm) were cleaned with acetone, ethanol and ultrapure water thoroughly under the condition of ultrasonication. The details of fabrication were as follows: Generally, 10 μL of 5 mg/mL B-TiO_2 NPs uniform suspension was coated onto the ITO pieces. On account of the B-TiO_2 NPs/ITO electrode, the BiOI NSs were modified on the mentioned electrode by a successive ionic layer adsorption and reaction (SILAR). Specifically, the BiOI NSs/B-TiO_2 NPs/ITO electrode was prepared by immersing the B-TiO_2 NPs/ITO electrode into 5 mM $Bi(NO_3)_3$ and 5 mM KI solutions for 10 s respectively and the electrode was washed with ultrapure water after each dipping step. The procedure was repeated several times. Then the BiOI NSs/B-TiO_2 NPs/ITO electrode was calcinated at 200 °C for 2 h in a muffle furnace. Next, 6 μL of Au NPs solution was spread onto the resulting BiOI NSs/B-TiO_2 NPs/ITO electrode. 6 μL of 5 μg/mL Ab_1 dropped onto the Au NPs/BiOI NSs/B-TiO_2 NPs/ITO electrode followed by rinsed with ultrapure water. After washed with 0.1 M PBS (pH 7.4) to remove the unbound Ab_1, 3 μL of 1% wt BSA solution was modified on the above electrode. Then 6 μL of different concentrations of PCT were incubated onto the resulting electrode. Rinsed with 0.1 M PBS (pH 7.4), 6 μL of 5 mg/mL PbS/Co_3O_4-Ab_2 was immobilized onto the above electrode through immunoreaction and washed with 0.1 M PBS (pH 7.4). The reaction time and reaction conditions of Ab_1, PCT and PbS/Co_3O_4-Ab_2 both were 1 h in the

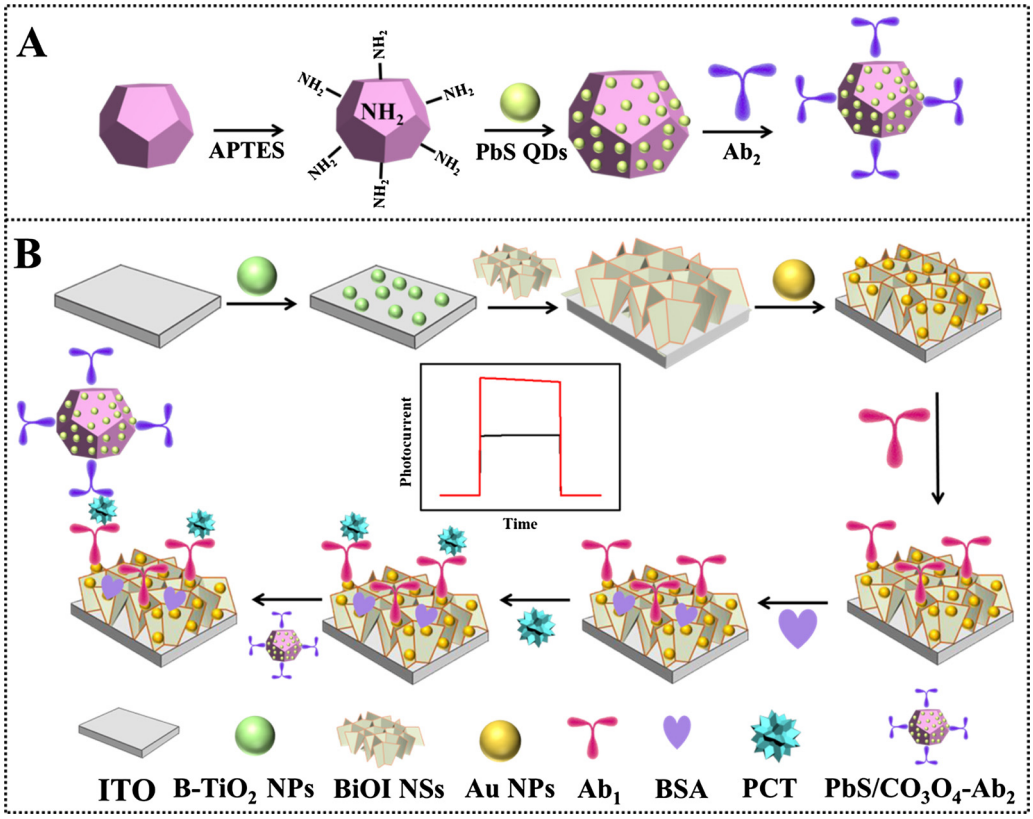

Scheme 1. (A) The preparation of PbS/Co_3O_4-Ab_2 and (B) fabrication process of the signal-off PEC immunosensor for PCT.

condition of 4 °C. Finally the PEC immunosensor was fabricated successfully.

2.5. PEC detection

I-t curves of PEC detection were carried out in the 0.1 mol/L phosphate-buffered solution (PBS) containing amount of AA with traditional three electrode system including the ITO slice as working electrode, Hg/Hg_2Cl_2 as reference electrode and the platinum wire electrode as counter electrode.

3. Results and discussion

3.1. Characterization of prepared materials

The X-ray diffraction (XRD) was used to characterize the crystalline phase of prepared materials as shown in Fig. 1A. The curve a (B-TiO_2 NPs) shows some peaks at 25.35, 37.78, 48.08, 55.11, 62.73, 75.09, corresponding to (101), (004), (200), (211), (204) and (215) of TiO_2 (JCPDS 04-0477). A number of conspicuous peaks (curve b) at 29.65, 31.65, 45.38, 51.35 and 55.15 were owing to the (102), (110), (200), (144) and (212) of BiOI NSs (JCPDS 04-0477), which suggested the desired hybrid was prepared successfully. In addition, the scanning electron microscope (SEM) images illustrated the morphology of B-TiO_2 NPs and BiOI NSs. It could be seen that B-TiO_2 NPs were aggregated nanoparticals (~20 nm in diameter) increasing the roughness of the ITO surface from Fig. 1B, which was conducive to the deposition of BiOI NSs. Fig. 1C displayed the BiOI NSs coating on the B-TiO_2 NPs were interlaced nanosheet structure with the high surface area. Further, the Au NPs loading on the BiOI NSs evenly was shown in Fig. 1D. Specifically, Au NPs are characterized by TEM and HRTEM images. Au NPs were uniform particle size from Fig. S4A and the size was about 15 nm as shown in Fig. S4B. Energy dispersive spectrometry (EDS) was utilized studying the elemental composition of the prepared materials. The results were shown in Fig. S1A that Ti, O, Bi, I, Au elements existed in the composite structure.

The morphology of signal labels was characterized by transmission electron microscopy (TEM) and SEM images. Fig. 1E displayed the fabricated PbS QD_S were evenly dispersed. As shown in Fig. 1F, the SEM image revealed that Co_3O_4 possessed uniform polyhedron structure with average size about 500 nm. It obviously noted in Fig. 1G that the surface of polyhedron changed rougher and was decorated with small particle substance, which illustrated that the PbS QD_S stuck to the Co_3O_4 polyhedron. In order to prove the successful synthesis of PbS/CO_3O_4, the element composition of the complex was measured with EDS (Fig. 1H) and the Pb, S, Co, O elements were clearly observed. Further notice, the XRD peaks (curve b) in Fig. S1B of PbS/CO_3O_4 had both characteristic peaks of Co_3O_4 polyhedron (curve a) and PbS QDs (curve b), which implied that the PbS/Co_3O_4 was prepared successfully to some extent.

The X-ray photoelectron spectroscopy (XPS) was utilized for the elemental analysis to confirm the truth about the success fabrication of PbS/CO_3O_4. In the full-survey XPS spectra (Fig. 2A), the existence of elements Co, O, Pb, and S can be confirmed. The high-resolution spectrum of Co 2p was shown in Fig. 2B. Two prominent peaks were shown at about 796 and 781 eV, which were assigned respectively to the Co $2p_{1/2}$and Co $2p_{3/2}$ peaks. Co $2p_{3/2}$, Co^{3+} (779.8 eV) and Co^{2+} (782.1 eV) were observed at the binding energy of around 781 eV, while Co $2p_{1/2}$, Co^{3+} (794.7 eV) and Co^{2+} (796.9 eV) was observed at the binding energy of about 796 eV as a shoulder peak [40,41]. O 1s peaks at 529.40 eV and 530.89 eV were shown in Fig. 2C owning to the lattice oxygen species and the O—H bonds of the surface adsorbed water [42,43]. The binding characteristic orbital energies of Pb $4f_{7/2}$ and Pb $4f_{5/2}$ were observed with peaks located at 138.3 and 143.2 eV in Fig. 2D [44], respectively. The S 2p peaks were shown in Fig. 2E at 161.8 and 167.63 eV belong to the S $2p_{1/2}$ and S $2p_{3/2}$ peaks [45]. C 1s peak was shown attributing to the hydrocarbon from the instrument in Fig. 2F.

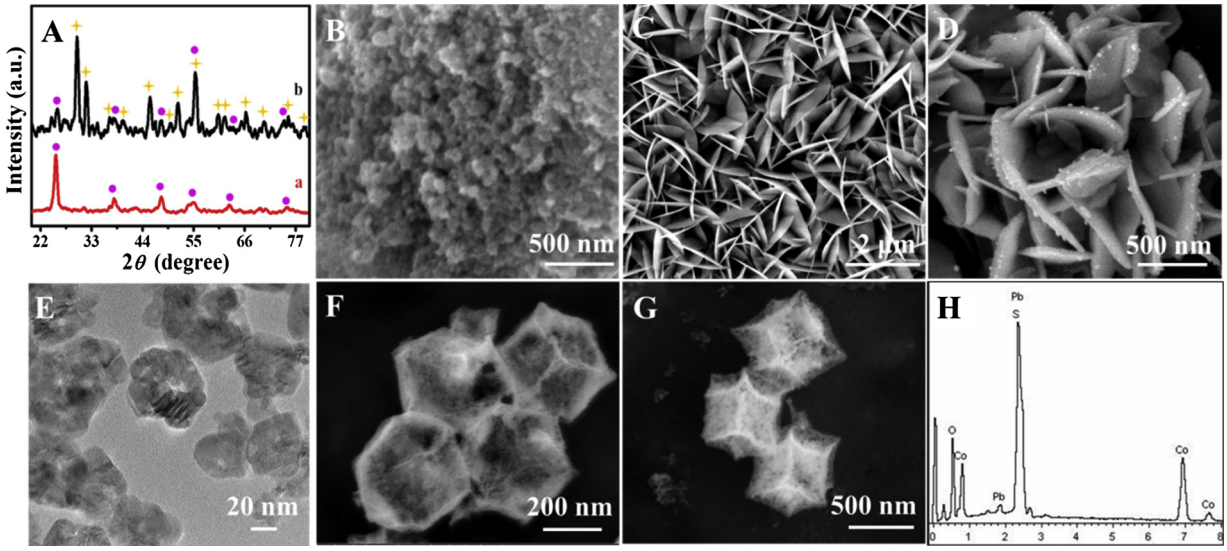

Fig. 1. (A) XRD spectrum of (a) B-TiO_2 NPs, (b) BiOI NSs/B-TiO_2 NPs; SEM images of (B) B-TiO_2 NPs, (C) BiOI NSs/B-TiO_2 NPs, and (D) Au NPs/BiOI NSs/B-TiO_2 NPs, respectively; (E) TEM image of PbS QDs; SEM images of (F) Co_3O_4 polyhedron and (G) PbS/Co_3O_4; (H) EDS spectrum of PbS/Co_3O_4.

3.2. Characterization and possible mechanism of the PEC immunosensor

Electrochemical impedance spectroscopy (EIS) has been a familiar way to analyze the interfacial properties of constructed electrode [46]. The acquired experiment results at different steps of the PEC immunosensor fabrication process were displayed in the Nyquist plots in Fig. 3A. The equivalent circuit of the system (the inset of Fig. 3A) contained the solution resistance (R_s), the electron transfer resistance (R_{et}), the Warburg impedance (Z_ω) and the double-layer capacitance (C_{dl}), which value were revealed in Table S1. Therein, the semicircle diameter of EIS was representative to the R_{et}. Specifically, the bare ITO electrode exhibited a smallest value (curve a). The increased R_{et} value was due to the poor conductivity of semiconductor after modifying of B-TiO_2 NPs and BiOI NSs (curve b and c). When Au NPs were loaded on the above electrode, the R_{et} value was decreased because of the excellent conductivity of Au NPs (curve d). With the immobilization of Ab_1 (curve e), the block of BSA (curve f), the incubation of PCT (curve g) and PbS/Co_3O_4-Ab_2 (curve h) in order, the R_{et} value enhanced gradually owing to the insulation of protein and the steric hindrance of material. In summary, the variation of R_{et} value was an advantageous proof for the successful construction of PEC immunosensor.

Additionally, a photocurrent comparison is an efficacious way to prove the construction process of proposed PEC immunosensor. The measurement results were illustrated in Fig. 3B. The photocurrent of bare ITO electrode (curve a) was close to zero. The photocurrent was relatively low after dropping the B-TiO_2 NPs onto the ITO electrode (curve b) because its large band gap reversely. The modification of BiOI NSs (curve c) caused the intensely enhancement of photocurrent signal, which was attributed to the narrow band gap of BiOI NSs and the cascade band-edge levels between B-TiO_2 NPs and BiOI NSs increasing the photocurrent conversion efficiency. The photocurrent was further increased after the loading of Au NPs (curve d) due to the excellent conductivity and LSPR effect making the rapidly transfer of photogenerated charge. After the incubation of Ab_1 (curve e), BSA (curve f)

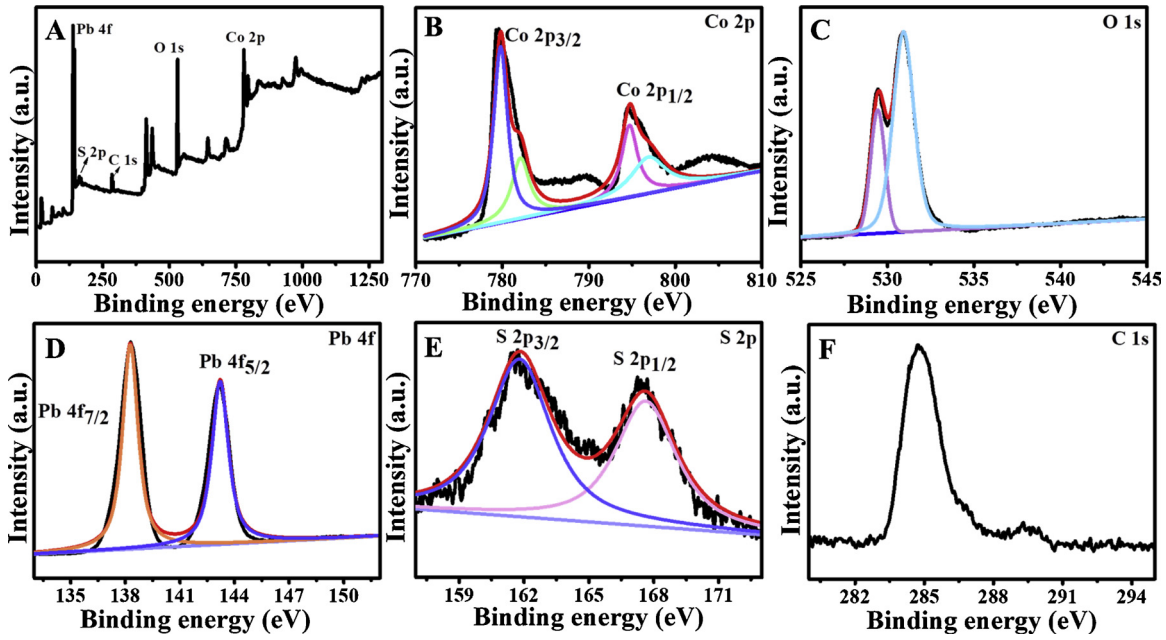

Fig. 2. (A) Full-survey XPS spectrum of PbS/CO_3O_4 and high-resolution XPS spectra of (B) Co 2p, (C) O 1s, (D) Pb 4f, (E) S 2p and (F) C 1s, respectively.

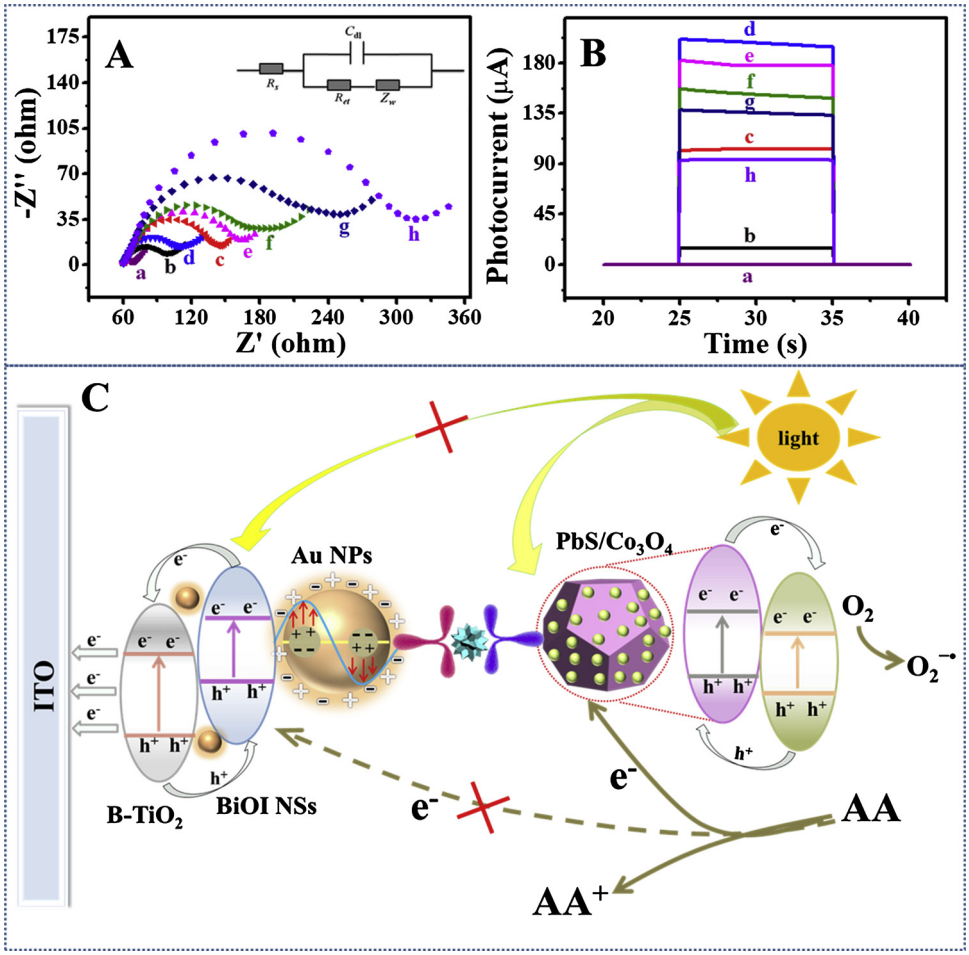

Fig. 3. (A) Nyquist plots of EIS and (B) photocurrent responses in the different stages of the electrode modification: (a) ITO, (b) ITO/B-TiO_2 NPs, (c) ITO/B-TiO_2 NPs/BiOI NSs, (d) ITO/B-TiO_2 NPs/BiOI NSs/Au NPs, (e) ITO/B-TiO_2 NPs/BiOI NSs/Au NPs/Ab_1, (f) ITO/B-TiO_2 NPs/BiOI NSs/Au NPs/Ab_1/BSA, (g) ITO/B-TiO_2 NPs/BiOI NSs/Au NPs/Ab_1/BSA/PCT, (h) ITO/B-TiO_2 NPs/BiOI NSs/Au NPs/Ab_1/BSA/PCT/(PbS/Co_3O_4-Ab_2); (C) The possible electron-transfer mechanism of the fabricated PEC immunosensor.

and PCT (curve g) onto the ITO/B-TiO_2 NPs/BiOI NSs/Au NPs electrode orderly, the photocurrent was reduced due to the insulation of protein for electron transport. Finally, the photocurrent response continued to decrease mightily because the hindrance effect and the competitive effect of PbS/Co_3O_4-Ab_2 (curve h). A serious of obvious photocurrent change represented the fabricated process of the proposed PEC immunosensor triumphantly.

Fig. 3C displayed the possible photogenerated charge transfer mechanism of the proposed immunosensor and Fig. S2 shown the photocurrent response due to the effect of difference substance. In the PEC immunosensor, B-TiO_2 NPs and BiOI NSs as photoactive matrix produce the photocurrent. Therein, B-TiO_2 NPs possessing the wider bandgap brought about a low photocurrent (curve a of Fig. S2). Coating on the BiOI NSs, the photocurrent was increased (curve b of Fig. S2) owing to two reasons: (a) the BiOI NSs as a flake-like narrow bandgap structure harvest more light and (b) the BiOI NSs and B-TiO_2 NPs formed the p-n heterojunction and the matched band gap accelerating charge transfer and inhibiting the recombination of photogernerated e^-/h^+ [47]. Specifically, B-TiO_2 NPs and BiOI NSs both produced e^-/h^+ under the light irradiation, photogenerated electron in the conduction band of BiOI NSs transfered to the conduction band of B-TiO_2 NPs, and AA as electron donor removed photogenerated holes in the valence band, increasing the photocurrent response. After dropping on the Au NPs, the photocurrent was continuously enhanced because of the effect of localized Surface Plasmon Resonance (LSPR) [48].

In addition, the signal label played an important role in the variation of photocurrent for a signal-off PEC immunosensor. The PbS/Co_3O_4 as bioconjugate owned the double inhabitation effect and the decreasing photocurrent of PbS/Co_3O_4 (curve g in Fig. S2) changed more obvious than Co_3O_4 polyhedron (curve e in Fig. S2) and PbS QDs (curve f in Fig. S2). The reasons were summarized as follows: (1) the PbS QDs that absorb full wavelength light competed with matrix for absorption of irradiation; (2) the steric resistance of Co_3O_4 obstructed the charge transfer and produced inhabitation for the contact between matrix and AA; (3) the PbS/Co_3O_4 formed the competition situation with matrix for AA as electron donor. Additionally, the Co_3O_4 and PbS QDs brought about the photogenerated e^-/h^+, the photogenerated electron in the conduction band of Co_3O_4 transfered to the conduction band of PbS QDs. Then the electron was reacted with the dissolved oxygen of electrolyte forming the superoxide anion radicals $(O^{2-})^{\cdot}$, which contended AA with matrix [49]. Based on the above factors, a double suppressive signal-off PEC platform was conducted.

3.3. Optimization of experimental conditions

Some experimental conditions were studied for improving performance of proposed PEC immunosensor, for example, the concentration of B-TiO_2 NPs, the SILAR cycles of BiOI NSs, the concentration of AA and the pH in the detection solution. B-TiO_2 NPs has an effect on the properties of the immunosensor and the optimization result was as shown in Fig. S3A. The photocurrent response was enhancive with the increasing concentration of B-TiO_2 NPs. And the value of photocurrent

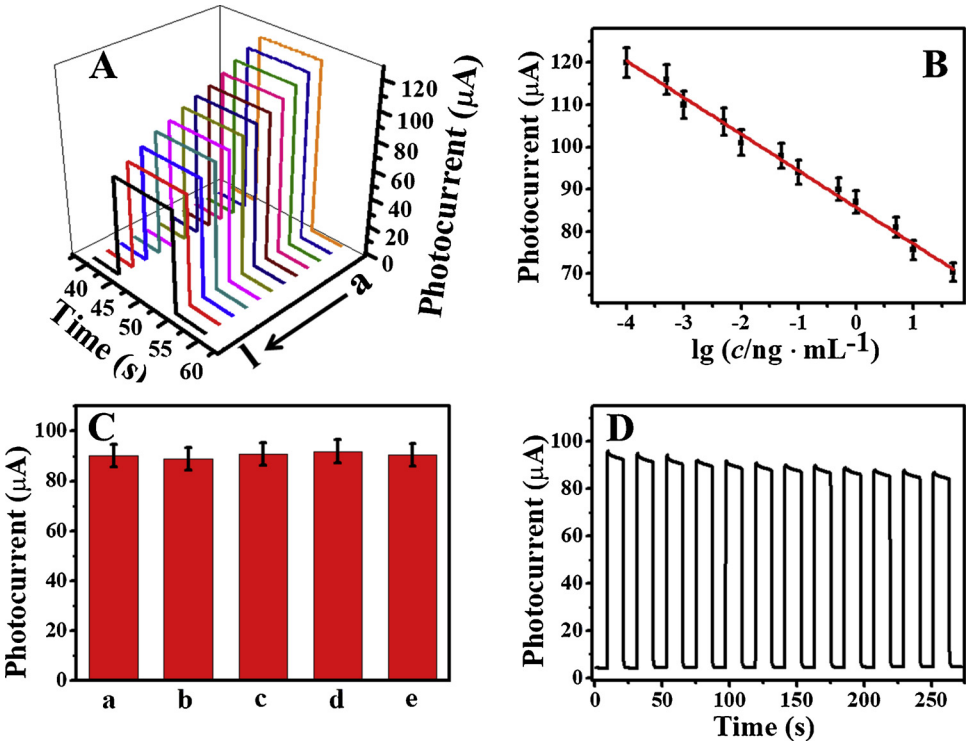

Fig. 4. (A) Photocurrent response curve and (B) Calibration curve of the PEC immunosensor for PCT detection from 0.1 pg/mL to 50 ng/mL :(a) 0.0001, (b) 0.0005, (c) 0.001, (d) 0.005, (e) 0.01, (f) 0.05, (g) 0.1, (h) 0.5, (i) 1, (j) 5, (k) 10, (l) 50 (Units: ng/mL); (C) Photocurrent signals of the PEC immunosensor toward (a) 0.5 ng/mL PCT without interfering species or 0.5 ng/mL PCT with 50 ng/mL (b) CEA, (c) PSA, (d) NT-pro BNP, (e) Aβ respectively; (D) Time-based photocurrent response of the PEC immunosensor under the irradiation on/off 12 times (c_{PCT} = 0.5 ng/mL).

was a plateau at 5 mg/mL B-TiO_2 NPs. The decreasing photocurrent was resulted from excess B-TiO_2 NPs blocking the charge transport. The SILAR cycles had an influence on the amount of BiOI NSs as a kind of main photoactive substance. It could be seen that the photocurrent enhanced as the increasing times of coating cycles in Fig. S3B. However, the downward tendency was occurred when the coating cycles were exceeded 30 due to the barrier effect [50]. The detection solution including the content of AA and pH was a critical factor for the properties of PEC immunosensor. On the hand, AA as an electron donor sweeping the holes inhabited the recombination of e^-/h^+ resulting in the enhancement of photocurrent response. At 0.1 mol/L AA the value of photocurrent reached the peak according to the Fig. S3C. On the other hand, pH affected deeply the photocurrent response. Too acidic or alkaline environment had an adverse impact on the activity of the protein [51]. Fig. S3D demonstrated that the PBS (pH 7.4) was suitable surroundings.

3.4. PEC detection for PCT

Different concentrations of PCT were detected under the optimized experimental condition using the proposed PEC immunosensor. Fig. 4A displayed the photocurrent variation of the PEC immunosensor with the change of PCT concentration. Obviously, the photocurrent was decreased as the PCT concentration increase, illustrating the photocurrent signal was interrelated highly with the concentration of PCT. And then, the specific relationship between photocurrent and PCT concentration was investigated. It could be seen that the logarithmic value of PCT concentration and photocurrent was favourable linear relationship when the PCT concentration was ranged from 0.1 pg/mL to 50 ng/mL in Fig. 4B. And the linear relation was I = 85.76–8.66 lg c with a correlation coefficient of 0.9921. Complementally, the detection limit for PCT was 0.02 pg/mL (S/N = 3). Making a comparison with reported works for detecting PCT, as summarized in Table S2, the performance of prepared PEC immunosensor was superior.

3.5. Selectivity, stability and reproducibility

Some interfering substances including carcino-embryonic antigen (CEA), prostate-specific antigen (PSA), amino-terminal pro-B-type natriuretic peptide (NT-pro BNP) and β-Amyloid oligomers (Aβ) were chosen as interfering substance to evaluate the selectivity of the prepared PEC immunosensor. The selectivity experiment carried out under the condition of 0.5 ng/mL PCT containing 50 ng/mL interfering substance respectively. The photocurrent results were shown in Fig. 4C and the added interfering substance caused tiny photocurrent changes demonstrating the excellent selectivity of proposed PEC immunosensor.

To assess the stability of the fabricated immunosensor, the photocurrent was recorded with the light irradiation on/off cycles with an interval of 10 s for 12 times as illustrated in Fig. 4D. The un-conspicuous photocurrent variation proved the immunosensor possessing the satisfactory stability.

Reproducibility played an important role in investigating the performance of PEC immunosensor. Thence, five consistent electrodes modified with 0.5 ng/mL PCT were measured in the same situation. Relative standard deviation (RSD) of the immunosensor was 1.47% indicating the good reproducibility of prepared PEC immunosensor.

3.6. Real sample analysis

The proposed PEC immunosensor was constructed for PCT detection though adding the different concentration solution to the human serum sample for evaluating the accuracy and feasibility. The measurement results were as illustrated in Table 1. The obtained recovery ranged from 96.8% to 101.3% and the RSD was in the range of 3.69–4.94%, which indicated the PEC immunosensor possessing the practicality and stupendous application potential for clinical diagnosis early.

4. Conclusion

In summary, an innovative signal-off PEC immunosensor was proposed for the detection biomolecules through the cooperation effect of Au NPs/BiOI NSs/B-TiO_2 NPs sensitization structure and the signal

Table 1
PCT determination in human serum sample by proposed PEC immunosensor.

Sample concentration (ng/mL)	Added contents (ng/mL)	Detection content (ng/mL)	RSD (%, n = 5)	Recovery (%)
0.56	0.25	0.83,0.85,0.78,0.75,0.80	4.94	96.8
	0.50	1.04,1.10,1.03,1.07,1.01	3.37	98.0
	2.00	2.65,2.48,2.58,2.71,2.51	3.69	101.3

amplification strategy based on PbS/Co_3O_4 quencher. Therein, Au NPs and BiOI NSs sensitized B-TiO_2 NPs enhancing the photocurrent response through increase the utilization of light source, accelerating the transfer of charge and preventing the photogenerated e^-/h^+ recombination. Furthermore, the PbS/Co_3O_4 as an excellent signal-off label weakened the photocurrent signal by the competition for light absorption and consuming AA with photoactive matrix and the steric impendence blocking the transfer of electron and AA. Taking advantage of the Au NPs/BiOI NSs/B-TiO_2 NPs sensitization structure as photoactive matrix and PbS/Co_3O_4 as signal label, the proposed signal-off PEC for detecting PCT with satisfactory selectivity, stability and reproducibility possessed the wide detection range and low detection limit. Hence, the signal-off PEC immunosensor opened up horizon for the biomolecules detection.

Acknowledgments

This study was supported by the National Key Scientific Instrument and Equipment Development Project of China (No. 21627809), National Natural Science Foundation of China (Nos. 21575050, 21777056, 21505051), Jinan Scientific Research Leader Workshop Project (2018GXRC024), National Natural Science Foundation of China (21602077), the Shandong Provincial Natural Science Foundation, China (2016ZRB01AHM).

Appendix A. Supplementary data

Supplementary material related to this article can be found, in the online version, at doi:https://doi.org/10.1016/j.snb.2019.127001.

References

[1] S.D. Carrigan, G. Scott, M. Tabrizian, Toward resolving the challenges of sepsis diagnosis, Clin. Chem. 50 (2004) 1301–1304.
[2] H. Li, Y. Sun, J. Elseviers, S. Muyldermans, S. Liu, Y. Wan, A nanobody-based electrochemiluminescent immunosensor for sensitive detection of human procalcitonin, Analyst 139 (2014) 3718–3721.
[3] Y. Sui, A. Xu, X. Jin, J. Zheng, X. He, Y. Cheng, et al., In situ enzymatic generation of gold for ultrasensitive amperometric sandwich immunoassay of procalcitonin, Biosens. Bioelectron. 117 (2018) 422–428.
[4] J. Wei, W. Chang, A. Qileng, W. Liu, Y. Zhang, S. Rong, et al., Dual-modal split-type immunosensor for sensitive detection of microcystin-LR: enzyme-induced photoelectrochemistry and colorimetry, Anal. Chem. 90 (2018) 9606–9613.
[5] H. Xue, J. Zhao, Q. Zhou, D. Pan, Y. Zhang, Y. Zhang, et al., Boosting the sensitivity of a photoelectrochemical immunoassay by using SiO2@polydopamine core–Shell nanoparticles as a highly efficient quencher, ACS Appl. Nano Mater. 2 (2019) 1579–1588.
[6] C. Sui, Y. Zhou, M. Wang, H. Yin, P. Wang, S. Ai, Aptamer-based photoelectrochemical biosensor for antibiotic detection using ferrocene modified DNA as both aptamer and electron donor, Sens. Actuators B: Chem. 266 (2018) 514–521.
[7] H.Y. Wang, C.L. Qi, W.H. He, M.H. Wang, W.J. Jiang, H.S. Yin, S.Y. Ai, A sensitive photoelectrochemical immunoassay of N^6–methyladenosine based on dual-signal amplification strategy: Ru doped in SiO_2 nanosphere and carboxylated g-C_3N_4, Biosens. Bioelectron. 99 (2018) 281–288.
[8] G.L. Wang, J.J. Xu, H.Y. Chen, S.Z. Fu, Label-free photoelectrochemical immunoassay for alpha-fetoprotein detection based on TiO_2/CdS hybrid, Biosens. Bioelectron. 25 (2009) 791–796.
[9] S.-Y. Yu, Y. Gao, F.-Z. Chen, G.-C. Fan, D.-M. Han, C. Wang, et al., Fast electrochemical deposition of CuO/Cu_2O heterojunction photoelectrode: Preparation and application for rapid cathodic photoelectrochemical detection of L-cysteine, Sens. Actuators B: Chem. 290 (2019) 312–317.
[10] L. Wang, W. Gu, P. Sheng, Z. Zhang, B. Zhang, Q. Cai, A label-free cytochrome c photoelectrochemical aptasensor based on CdS/$CuInS_2$/Au/TiO_2 nanotubes, Sens. Actuators B: Chem. 281 (2019) 1088–1096.
[11] J. Du, M. Liu, X. Lou, T. Zhao, Z. Wang, Y. Xue, et al., Highly sensitive and selective chip-based fluorescent sensor for mercuric ion: development and comparison of turn-on and turn-off systems, Anal. Chem. 84 (2012) 8060–8066.
[12] M.J. Li, Y.N. Zheng, W.B. Liang, R. Yuan, Y.Q. Chai, Using p-type PbS quantum dots to quench photocurrent of Fullerene-Au NP@MoS_2 composite structure for ultrasensitive photoelectrochemical detection of ATP, ACS Appl. Mater. Interface 9 (2017) 42111–42120.
[13] J. Gong, T. Fang, D. Peng, A. Li, L. Zhang, A highly sensitive photoelectrochemical detection of perfluorooctanic acid with molecularly imprined polymer-functionalized nanoarchitectured hybrid of AgI-BiOI composite, Biosens. Bioelectron. 73 (2015) 256–263.
[14] J. Wu, Y. Chen, M. Yang, Y. Wang, C. Zhang, M. Yang, et al., Streptavidin-biotin-peroxidase nanocomplex-amplified microfluidics immunoassays for simultaneous detection of inflammatory biomarkers, Anal. Chim. Acta 982 (2017) 138–147.
[15] K. Yan, Y. Liu, Y. Yang, J. Zhang, A cathodic "signal-off" photoelectrochemical aptasensor for ultrasensitive and selective detection of oxytetracycline, Anal. Chem. 87 (2015) 12215–12220.
[16] C. Ye, M.Q. Wang, H.Q. Luo, N.B. Li, Label-free photoelectrochemical "off-on" platform coupled with G-wire-enhanced strategy for highly sensitive microRNA sensing in cancer cells, Anal. Chem. 89 (2017) 11697–11702.
[17] W.W. Zhao, Z.Y. Ma, P.P. Yu, X.Y. Dong, J.J. Xu, H.Y. Chen, Highly sensitive photoelectrochemical immunoassay with enhanced amplification using horseradish peroxidase induced biocatalytic precipitation on a CdS quantum dots multilayer electrode, Anal. Chem. 84 (2012) 917–923.
[18] Y. Zhou, M. Wang, Z. Yang, H. Yin, S. Ai, A Phos-tag-based photoelectrochemical biosensor for assay of protein kinase activity and inhibitors, Sens. Actuators B: Chem. 206 (2015) 728–734.
[19] W.J. Jiang, L.N. Wu, J.L. Duan, H.S. Yin, S.Y. Ai, Ultrasensitive electrochemiluminescence immunosensor for 5-hydroxymethylcytosine detection based on Fe_3O_4@SiO_2 nanoparticles and PAMAM dendrimers, Biosens. Bioelectron. 99 (2018) 660–666.
[20] R. Chen, J. Wang, Y. Xia, L. Xiang, Near infrared light enhanced room-temperature NO_2 gas sensing by hierarchical ZnO nanorods functionalized with PbS quantum dots, Sens. Actuators B: Chem. 255 (2018) 2538–2545.
[21] R.N. Wang, S.B. Chen, Y.H. Ng, Q.Z. Gao, S.Y. Yang, S.Q. Zhang, F. Peng, Y.P. Fang, S.S. Zhang, ZnO/CdS/PbS nanotube arrays with multi-heterojunctions for efficient visible-light-driven photoelectrochemical hydrogen evolution, Chem. Eng. J. 362 (2019) 658–666.
[22] J.L. Liu, Z.L. Tang, Y. Zhuo, Y.Q. Chai, R. Yuan, Ternary electrochemiluminescence system based on rubrene microrods as luminophore and Pt nanomaterials as coreaction accelerator for ultrasensitive detection of microRNA from cancer cells, Anal. Chem. 89 (2017) 9108–9115.
[23] J. Wang, H. Han, X. Jiang, L. Huang, L. Chen, N. Li, Quantum dot-based near-infrared electrochemiluminescent immunosensor with gold nanoparticle-graphene nanosheet hybrids and silica nanospheres double-assisted signal amplification, Anal. Chem. 84 (2012) 4893–4899.
[24] Y. Zhang, Z. Jin, H. Yuan, G. Wang, B. Ma, Well-regulated nickel nanoparticles functional modified ZIF-67 (Co) derived Co_3O_4/CdS p-n heterojunction for efficient photocatalytic hydrogen evolution, Appl. Surf. Sci. 462 (2018) 213–225.
[25] R. Yang, K. Zou, Y. Li, L. Meng, X. Zhang, J. Chen, Co_3O_4-Au polyhedra: a multifunctional signal amplifier for sensitive photoelectrochemical assay, Anal. Chem. 90 (2018) 9480–9486.
[26] H. Mao, Y. Yan, N. Hao, Q. Liu, J. Qian, S. Chen, et al., Dual signal amplification coupling dual inhibition effect for fabricating photoelectrochemical chlorpyrifos biosensor, Sens. Actuators B: Chem. 238 (2017) 239–248.
[27] Y. Zhao, J. Gong, X. Zhang, R. Kong, F. Qu, Enhanced biosensing platform constructed using urchin-like ZnO-Au@CdS microspheres based on the combination of photoelectrochemical and bioetching strategies, Sens. Actuators B: Chem. 255 (2018) 1753–1761.
[28] C. Zhang, H. Yu, Y. Li, Y. Gao, Y. Zhao, W. Song, et al., Supported noble metals on hydrogen-treated TiO_2 nanotube arrays as highly ordered electrodes for fuel cells, ChemSusChem 6 (2013) 659–666.
[29] X. Li, L.S. Zhu, Y.L. Zhou, H.S. Yin, S.Y. Ai, Enhanced photoelectrochemical method for sensitive detection of protein kinase a activity using TiO_2/g-C_3N_4, PAMAM dendrimer, and alkaline phosphatase, Anal. Chem. 89 (4) (2017) 2369–2376.
[30] X. Lu, G. Wang, T. Zhai, M. Yu, J. Gan, Y. Tong, et al., Hydrogenated TiO_2 nanotube arrays for supercapacitors, Nano Lett. 12 (2012) 1690–1696.
[31] M.H. Wang, H.S. Yin, Y.L. Zhou, C.J. Sui, Y. Wang, X.J. Meng, S.Y. Ai, et al., Photoelectrochemical biosensor for microRNA detection based on a MoS_2/g-C_3N_4/black TiO_2 heterojunction with Histostar@AuNPs for signal amplification, Biosens. Bioelectron. 128 (2019) 137–143.
[32] S.G. Ullattil, S.B. Narendranath, S.C. Pillai, P. Periyat, Black TiO_2 nanomaterials: a review of recent advances, Chem. Eng. J. 343 (2018) 708–736.
[33] R.N. Wang, M. Zu, S.Y. Yang, S.Q. Zhang, W.Y. Zhou, Z.Y. Mai, C.Y. Ge, Y.H. Xu, Y.P. Fang, S.S. Zhang, Visible-light-driven photoelectrochemical determination of Cu^{2+} based on CdS sensitized hydrogenated TiO_2 nanorod arrays, Sens. Actuators

B: Chem. 270 (2018) 270–276.
[34] B. Zhang, H. Wang, H. Ye, B. Xu, F. Zhao, B. Zeng, Reversible redox mechanism based synthesis of plasmonic WO_3/Au photocatalyst for selective and sensitive detection of ultra-micro Hg^{2+}, Sens. Actuators B: Chem. 273 (2018) 1435–1441.
[35] Y.F. Ruan, N. Zhang, Y.C. Zhu, W.W. Zhao, J.J. Xu, H.Y. Chen, Photoelectrochemical bioanalysis platform of gold nanoparticles equipped perovskite Bi_4NbO_8Cl, Anal. Chem. 89 (2017) 7869–7875.
[36] G.L. Wang, K.L. Liu, J.X. Shu, T.T. Gu, X.M. Wu, Y.M. Dong, et al., A novel photoelectrochemical sensor based on photocathode of PbS quantum dots utilizing catalase mimetics of bio-bar-coded platinum nanoparticles/G-quadruplex/hemin for signal amplification, Biosens. Bioelectron. 69 (2015) 106–112.
[37] J. Xue, L. Yang, H. Wang, T. Yan, D. Fan, R. Feng, et al., Quench-type electrochemiluminescence immunosensor for detection of amyloid beta-protein based on resonance energy transfer from luminol@SnS_2-Pd to Cu doped WO_3 nanoparticles, Biosens. Bioelectron. 133 (2019) 192–198.
[38] J. Shao, Z. Wan, H. Liu, H. Zheng, T. Gao, M. Shen, et al., Metal organic frameworks-derived Co_3O_4 hollow dodecahedrons with controllable interiors as outstanding anodes for Li storage, J. Mater. Chem. A 2 (2014) 12194–12200.
[39] H. Tan, Z. Zhao, M. Niu, C. Mao, D. Cao, D. Cheng, et al., A facile and versatile method for preparation of colored TiO_2 with enhanced solar-driven photocatalytic activity, Nanoscale 6 (2014) 10216–10223.
[40] Y. Lu, W. Zhan, Y. He, Y. Wang, X. Kong, Q. Kuang, et al., MOF-templated synthesis of porous Co_3O_4 concave nanocubes with high specific surface area and their gas sensing properties, ACS Appl. Mater. Interface 6 (2014) 4186–4195.
[41] R. Zhang, T. Zhou, L. Wang, T. Zhang, Metal-organic frameworks-derived hierarchical Co_3O_4 structures as efficient sensing materials for acetone detection, ACS Appl. Mater. Interface 10 (2018) 9765–9773.
[42] W. Xu, W. Xie, Y. Wang, Co3O4-x-Carbon@Fe2-yCoyO3 heterostructural hollow polyhedrons for the oxygen evolution reaction, ACS Appl. Mater. Interface 9 (2017) 28642–28649.
[43] Y. Guo, Y. Dai, W. Zhao, H. Li, B. Xu, C. Sun, Highly efficient photocatalytic degradation of naphthalene by Co_3O_4/$Bi_2O_2CO_3$ under visible light: a novel p–n heterojunction nanocomposite with nanocrystals/lotus-leaf-like nanosheets structure, Appl. Catal. B: Environ. 237 (2018) 273–287.
[44] W.X. Dai, L. Zhang, W.W. Zhao, X.D. Yu, J.J. Xu, H.Y. Chen, Hybrid PbS quantum dot/nanoporous NiO film nanostructure: preparation, characterization, and application for a self-powered cathodic photoelectrochemical biosensor, Anal. Chem. 89 (2017) 8070–8078.
[45] W. Cui, M. Shao, L. Liu, Y. Liang, D. Rana, Enhanced visible-light-responsive photocatalytic property of PbS-sensitized $K_4Nb_6O_{17}$ nanocomposite photocatalysts, Appl. Surf. Sci. 276 (2013) 823–831.
[46] J. Feng, F. Li, X. Li, X. Ren, D. Fan, D. Wu, et al., An amplification label of core–shell CdSe@CdS QD sensitized GO for a signal-on photoelectrochemical immunosensor for amyloid β-protein, J. Mater. Chem. B 7 (2019) 1142–1148.
[47] W.W. Zhao, S. Shan, Z.Y. Ma, L.N. Wan, J.J. Xu, H.Y. Chen, Acetylcholine esterase antibodies on BiOI nanoflakes/TiO_2 nanoparticles electrode: a case of application for general photoelectrochemical enzymatic analysis, Anal. Chem. 85 (2013) 11686–11690.
[48] R. Zeng, L. Zhang, L. Su, Z. Luo, Q. Zhou, D. Tang, Photoelectrochemical bioanalysis of antibiotics on rGO-Bi_2WO_6-Au based on branched hybridization chain reaction, Biosens. Bioelectron. 133 (2019) 100–106.
[49] X. Wang, P. Gao, T. Yan, R. Li, R. Xu, Y. Zhang, et al., Ultrasensitive photoelectrochemical immunosensor for insulin detection based on dual inhibition effect of CuS-SiO_2 composite on CdS sensitized C-TiO_2, Sens. Actuators B: Chem. 258 (2018) 1–9.
[50] S.Y. Yu, L.P. Mei, Y.T. Xu, T.Y. Xue, G.C. Fan, D.M. Han, et al., Liposome-mediated in situ formation of AgI/Ag/BiOI Z-scheme heterojunction on foamed nickel electrode: a proof-of-concept study for cathodic liposomal photoelectrochemical bioanalysis, Anal. Chem. 91 (2019) 3800–3804.
[51] X. Li, Y. Wang, L. Shi, H. Ma, Y. Zhang, B. Du, et al., A novel ECL biosensor for the detection of concanavalin A based on glucose functionalized $NiCo_2S_4$ nanoparticles-grown on carboxylic graphene as quenching probe, Biosens. Bioelectron. 96 (2017) 113–120.

Yanrong Qian studies in school of chemistry and chemical engineering, University of Jinan as postgraduate student.

Jinhui Feng studies in school of chemistry and chemical engineering, University of Jinan as doctoral student.

Huan Wang received Ph.D. degree from China university of Geosciences (Beijing). Now, he is an associate professor at University of Jinan. His main research interests are the determination of electrochemical immunosensor.

Dawei Fan received Ph.D. degree from Lanzhou Institute of Chemical Physics, Chinese Academy of Sciences in 2010. Now, she is an associate professor at University of Jinan. Her main research interests are the determination of photoelectrochemical immunosensor.

Na Jiang received her PhD degree in Applied Chemistry from Dalian University of Technology in 2015 and took up a position as a docent in the University of Jinan in the same year. Her research interests are mainly in the synthesis of long wavelength fluorescent dyes and the development of fluorescent sensors for detecting polarity.

Qin Wei, a professor and DSc, has devoted herself to analytical teaching and scientific research. Her main research interests are the determination of protein and nucleic acid by photometry and the electrochemical immunosensor preparation. She has published over two hundred articles on analysis, immunosensor and applied successfully for many research projects, such as *Biomaterials, Advanced Functional Materials., Biosensors & Bioelectronics, Sensors and Actuators B-Chemical ACS Applied Materials & Interfaces, and Talanta*.

Huangxian Ju received his BS, MS and PhD degrees from Nanjing University during 1982–1992. He was a postdoc in Montreal University (Canada) in 1996–1997 and a guest professor in three universities of Germany and Ireland in 1999–2000. He became an associate and full professor of Nanjing University in 1993 and 1999. He is currently the director of State Key Laboratory of Analytical Chemistry for Life Science. His research interests focus on analytical biochemistry, biosensing and molecular diagnosis. He has published 635 papers in different journals with h-index of 85 (Google Scholar h-index 95 with about 31,634 citations).